



OPEN

Tamoxifen induces hypercoagulation and alterations in ER α and ER β dependent on breast cancer sub-phenotype *ex vivo*

K. Pather[✉] & T. N. Augustine[✉]

Tamoxifen shows efficacy in reducing breast cancer-related mortality but clinically, is associated with increased risk for thromboembolic events. We aimed to determine whether breast tumour sub-phenotype could predict propensity for thrombosis. We present two *ex vivo* Models of Tamoxifen-therapy, Model 1 in which treatment recapitulates accumulation within breast tissue, by treating MCF7 and T47D cells directly prior to exposure to blood constituents; and Model 2 in which we recreate circulating Tamoxifen by treating blood constituents prior to exposure to cancer cells. Blood constituents included whole blood, platelet-rich plasma and platelet-poor plasma. Hypercoagulation was assessed as a function of thrombin activity, expression of CD62P and CD63 activation markers defined as an index of platelet activation, and platelet morphology; while oestrogen receptor expression was assessed using immunocytochemistry with quantitative analysis. We determined, in concert with clinical studies and contrary to selected laboratory investigations, that Tamoxifen induces hypercoagulation, dependent on sub-phenotypes, with the T47D cell line capacity most enhanced. We determined a weak positive correlation between oestrogen receptor expression, and CD62P and CD63; indicating an association between tumour invasion profiles and hypercoagulation, however, other yet unknown factors may play a predictive role in defining hypercoagulation.

Breast cancer is one of the most commonly diagnosed cancers, accounting for 24.2% of 8.6 million new cases in women worldwide^{1,2}. Targeted treatment strategies, including Tamoxifen, a selective oestrogen receptor modulator (SERM) for hormone-dependent breast tumours, show efficacy in reducing mortality and increasing survival^{3,4}. Tamoxifen can be taken orally or intravenously, depending on the severity, staging and patient preference⁵, and is known to increase a patient's risk for thrombosis^{6,7}. Tamoxifen used as an adjuvant treatment strategy for breast cancers in post-menopausal women, indicated positive disease-free state with an associated greater risk for development of venous thromboembolisms (VTE)⁷⁻⁹. While Tamoxifen has shown efficacy in reducing mortality and increasing survival in patients^{1-4,10-13}, associated and resulting thrombosis remains the second main cause of mortality^{1,8-11,14}. This induction of hypercoagulation indicates an interplay between oestrogen-induced platelet activation as well as activation due to the cytotoxic nature of Tamoxifen itself¹⁵⁻¹⁷. The precise mechanism by which Tamoxifen exerts its procoagulant effect remains to be discovered^{7,18}; however, studies implicate the anti-oestrogenic activity of the drug on oestrogen receptor alpha (ER α), particularly on those expressed by platelets, to further increase the risk of VTE^{19,20}, and further effects on Factor VIII in promoting thrombotic events via its role in platelet activation¹⁸.

Platelets are key players in hypercoagulation and their role in tumour progression is becoming increasingly evident. Tumour cells facilitate platelet activation and aggregation, and the formation of a fibrin-rich network, by either direct contact with platelets or by the release of agonists including tissue factor, ADP, thrombin or thromboxane A2 (TXA2)^{21,22}. Of these agonists, thrombin is proposed to be the most potent contributor to platelet activation acting via engagement of platelet protease-activated receptors (PAR1-4) and ultimately inducing the coagulation cascade²³⁻²⁵. In turn, intratumoral platelets facilitate the acquisition of a more invasive phenotype in preparation for tumour cell intravasation and subsequent metastasis²⁶⁻²⁸. In the circulation, platelets form

School of Anatomical Sciences, Faculty of Health Sciences, University of the Witwatersrand, 7York Road, Parktown, Johannesburg 2193, South Africa. ✉email: kyrta.pather@wits.ac.za; tanya.augustine@wits.ac.za

heterotypic aggregates with tumour cells, shielding them from immune surveillance and high velocity shear forces, and facilitating extravasation to secondary sites while providing a rich source of growth factors^{25,26,29}.

Investigating these interactions *ex vivo* is fundamental to understanding the association with hypercoagulation and tumour progression, considering firstly, treatment strategies and secondly, sub-phenotypes that clinically would fall under the same phenotype. We have previously shown *in vitro* that Tamoxifen pre-treatment of breast cancer cell lines augments their ability to induce platelet activation³⁰ echoing clinical results^{17,31}. However, our results have contrasted with laboratory studies where Tamoxifen either administered to patients or Tamoxifen pre-treatment of blood *in vitro* conversely inhibited platelet activation^{32,33}. These contrasts are likely due to variance in methodological approaches and encourages further investigations. Clinically, Tamoxifen is administered orally or intravenously (IV), depending on the severity, staging and patient preference; allowing for availability within the circulation as well as ultimate accumulation of the therapy at the tumour site^{5,34}. In order to mimic these scenarios, in this study we present two co-culture models making use of blood constituents (whole blood, platelet-rich plasma and platelet-poor plasma) and breast cancer cell lines (MCF-7 and T47D): in Model 1, breast cancer cell lines were treated with a physiological dose of Tamoxifen prior to exposure to untreated blood constituents; whereas in Model 2, blood was treated with Tamoxifen prior to exposure to untreated breast cancer cell lines. This allowed us to investigate hypercoagulation as defined by thrombin release and generation by breast cancer cells with ensuing effects on platelet activation identified by CD62P/P-selectin and lysosome membrane protein 3 (LAMP3)/CD63 expression, with corresponding platelet morphological alterations.

Additionally, we previously identified that breast cancer cell lines, MCF-7 and T47D, differentially induced platelet activation under Tamoxifen treatment³⁰. Since these cell lines both correspond to the clinical luminal A subtype where ER and progesterone receptor (PR) expression is evident^{35,36}, this was not entirely expected. Since ER status is predictive of better prognosis following treatment^{37–39}, we investigated whether the ERs, ER α , most commonly studied^{37,40} and ER β , considered as predictive marker of Tamoxifen resistance in breast tumours yet not clinically assessed^{41–43}, showed any association with markers of hypercoagulation that could hold predictive value for thrombotic propensity relative to tumour phenotype.

Results

Non-tumorigenic breast epithelial cell line MCF10A induces low levels of coagulation and alters ER expression on exposure to blood.

Co-incubation of blood constituents with MCF10A cells did not induce significant changes in IPA of either activation marker overall or per interval gate (Fig. 1a,b); except for (WB) CD63 IPA in I5 (Fig. 1b). Morphologically, platelets from untreated WB showed inactive platelets in resting phase (Fig. 1c-A); while platelets from thrombin-treated WB indicated activity, with the presence of membrane folds and extending filipodia (Fig. 1c-B). WB platelets exposed to MCF10A breast epithelial cells were mostly in resting phase, with some showing a smooth membrane with few surface folds and filipodia (Fig. 1c-C), however, this was lower than that of Tamoxifen-treated WB (Fig. 1c-D). This corresponds with detected thrombin levels which reflect that found in WB, since little to no levels of thrombin were detected in MCF10A-conditioned culture media (Fig. 1d). When PRP- (Fig. 1c-E) and PPP- (Fig. 1c-I), which are subjected to centrifugation steps concentrating fibrinogen, were exposed to MCF10A cells, fibrin plaque formation was evident (Fig. 1c-G,J), greater than that noted in the positive PRP control (Fig. 1c-F) and Tamoxifen-treated PRP (Fig. 1c-H) and PPP (Fig. 1c-K), explaining the reduction in detectable thrombin in these culture groups (Fig. 1d). In response to co-incubation with blood constituents, MCF10A cells changed from a typical epithelial morphology (Fig. 1e-A) to a star-shaped, elongated cell (Fig. 1e-B–D). Imaging cells showed higher ER α (green fluorescence) and lower ER β (red fluorescence) concentrated within the nucleus on exposure to PRP and PPP (Fig. 1e-C,D), while exposure to WB increased cytoplasmic ER β (Fig. 1e-B) (DAPI nuclear stain not shown since it obscures nuclear ER expression). This was verified quantitatively, with some variable expression in response to blood constituents (Fig. 1f).

PRP presents with higher thrombin concentration and platelets in later stages of activation than WB, but remain responsive to induced coagulation.

Baseline levels of platelet activation were determined by thrombin activity (Fig. 2), IPA (Table 1) and platelet ultrastructure. Thrombin activity assessment of blood constituent control samples indicated baseline levels of thrombin availability in WB at 41.7 ng/mL \pm 3.58 (Fig. 2). PPP had a slightly decreased level of thrombin availability, at 40.4 ng/mL \pm 2.37; and was assayed for the presence of platelet microparticles; expressing CD62P IPA at 1.44E+05 \pm 2.04E+05 and CD63 IPA 5.35E+05 \pm 3.00E+05. PRP indicated significantly ($p < 0.05$; $p = 1.73E-06$) greater levels of thrombin availability 47.7 ng/mL \pm 1.01E+03. This reflects the significantly higher early stage (CD62P, released initially from α granules) and late stage (CD63, released later from δ granules) compared to WB as expected, given centrifugation steps (Table 1). A ratio between CD62P IPA and CD63 IPA was used to explain the capacity of platelets to progress to later stages of activation; where a lower ratio indicated a later stage as well as a greater spread throughout interval gates (Supplementary Tables S1, S2), as identified in PRP. This was also evident in micrographs (Fig. 1c-E). This concept is further noted in the positive controls, where the addition of suprathreshold thrombin to WB induced only slightly higher overall CD62P but significantly higher CD63 IPA (Table 1). Thrombin availability increased only slightly ($p > 0.05$) and this could be attributed to the binding of the exogenous thrombin to the platelets within the WB itself (Fig. 2). The addition of thrombin to PRP as a positive control; however, significantly heightened levels of thrombin availability ($p = 1.17E-06$), much higher than the detectable levels of the assay itself, resulting in a negative value of -45.8 ng/mL \pm 2.29E+02^{44,45}. Since PRP contains high numbers of platelets this allows for interaction rates with thrombin to be heightened as platelet activation proceeds (Fig. 2). Platelets at this heightened level of expression lose CD62P, however, CD63 persists, reflecting hypercoagulation

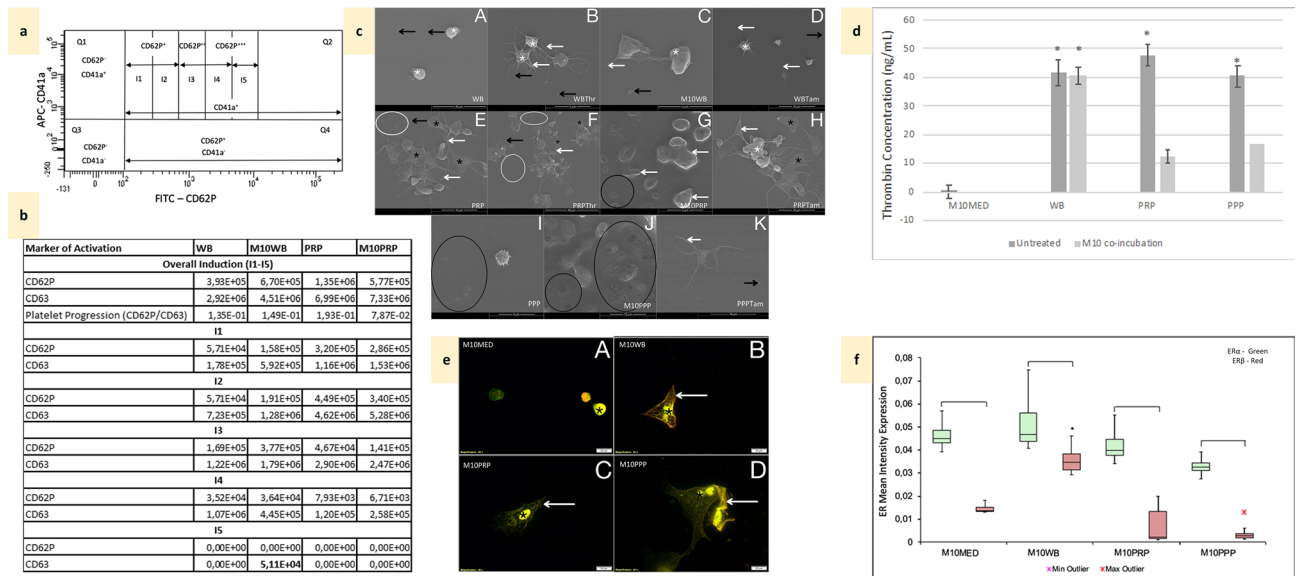


Figure 1. Controls; non-tumorigenic cell line MCF10A effects on coagulation and ER expression and Platelet ultrastructural alterations in Tamoxifen-treated blood constituents compared to controls. *WB* untreated whole blood, *M10WB* WB co-incubated with MCF10A cells, *PRP* untreated platelet-rich plasma, *M10PRP* PRP co-incubated with MCF10A cells, *PPP* Platelet-poor plasma, *M10PPP* PPP co-incubated with MCF10A cells, *M10MED* untreated MCF10A cells (media control). **(a)** Scatterplot diagram showing platelet activation (CD62P or CD63) across defined interval gates. **(b)** Index of platelet activation (IPA) for CD62P and CD63, in blood constituents exposed to MCF10A cells. Overall and per interval gate levels. Bold: significantly ($p < 0.05$) different to matched control groups. **(c)** Platelet ultrastructural alterations. White*—membrane folds, black*—hyalomere spread, white arrow—extending filipodia, black arrow—microparticles, white circle—fibrin, black circle—fibrin clots with pores/plaques **A:** *WB*—inactive platelets with smooth membrane. **B:** *WBThr* Positive control *WB* (0.1 U/mL thrombin)—active platelets with membrane folds and extending filipodia. **C:** *M10WB* slightly active platelets. **D:** *WBTam* Tamoxifen-treated *WB*—active platelets with membrane folds, filipodia extensions and few microparticles **E:** *PRP*—spread platelets with pores, extending filipodia and fibrin **F:** *PRPThr* Positive control *PRP* (0.1 U/mL thrombin)—spread platelets aggregating, filipodia extension and fibrin formation. **G:** *M10PRP*—fibrin plaque formation with pores. **H:** *PRPTam* Tamoxifen-treated *PRP*—spread platelets aggregating, membrane budding, lamellipodia and filipodia extension. **I:** *PPP*—crenated red blood cells, platelet remnants and fibrin clots. **J:** *M10PPP*—fibrin plaque formation with pores. **K:** *PPPTam* Tamoxifen-treated *PPP*—scattered yet active platelets. **(d)** Thrombin concentrations $*p < 0.05$ compared to untreated MCF10A. **(e)** Co-localisation of ER α (green) and ER β (red) in MCF10A cells. **A:** *M10MED*—nuclear ER α and ER β , no cytoplasmic staining. **B:** *M10WB*—primarily nuclear ER α and cytoplasmic ER β . **C:** *M10PRP*—nuclear (*) and cytoplasmic (white arrow) ER α expression. Low ER β expression. **D:** *M10PPP*—high nuclear ER α and low ER β in cytoplasm. **(f)** Box and whisker plots representing quantitative analysis of ER α (green) and ER β (red) expression in MCF10A cells, following exposure to blood constituents; *significant ($p < 0.05$) differences compared to untreated MCF10A.

(Table 1). Morphologically this is seen as platelet aggregation, with spread platelets, filipodia extension, and more microparticles and fibrin formation (Fig. 1c–f).

Breast cancer cell lines induce a hypercoagulatory environment. Assessment of thrombin generation showed that control, untreated breast cancer cells secreted more thrombin; MCF7 $37.77 \text{ ng/mL} \pm 4.00\text{E}+01$; T47D $41.61 \text{ ng/mL} \pm 1.01\text{E}+03$, than the non-tumorigenic MCF10A cells; $0.073 \text{ ng/mL} \pm 6.59\text{E}+01$ (Figs. 1d, 2). MCF7 cells generated significantly less thrombin than the WB control ($p = 7.08\text{E}-17$); however, MCF7 cells exposed to WB increased the level of detectable thrombin significantly ($p = 1.17\text{E}-06$) when compared to untreated MCF7 cells. This greater level of available thrombin could be due to low levels of platelet activation evident in untreated WB (Fig. 3a–A). However, when PRP and PPP were exposed to MCF7 cells, slight decreases in detectable thrombin levels is noted compared to matched blood constituents (Fig. 2), possibly due to platelet activation within the concentrated PRP as well as the generation of fibrin in both samples (Fig. 3a–C,E). T47D cells secreted thrombin at $41.61 \text{ ng/mL} \pm 1.01\text{E}+03$ which lowered significantly ($p = 1.30\text{E}-06$) when cells were exposed to blood constituents (Fig. 2), attributable to platelet ligation and subsequent activation. Both breast cancer cell lines induced higher CD62P and CD63 IPA in WB than the non-tumorigenic MCF10A cell line ($p > 0.05$); with MCF7 cells inducing significantly higher CD62P, and T47D cells induced significantly more CD63 IPA, compared to WB (Table 1). Matched diluent control-induction of IPA (Table 1) and thrombin generation was not different to untreated cell lines (Fig. 2), and platelets remained in early stages of activation (Figs. 3a–B,D,F, 4a–B,D,F). In PRP, a consistently higher level of platelet activation was noted. PRP exposed to MCF7 cells (Table 2) showed an increase in CD62P IPA and CD63 IPA, shifting to later stages of activation

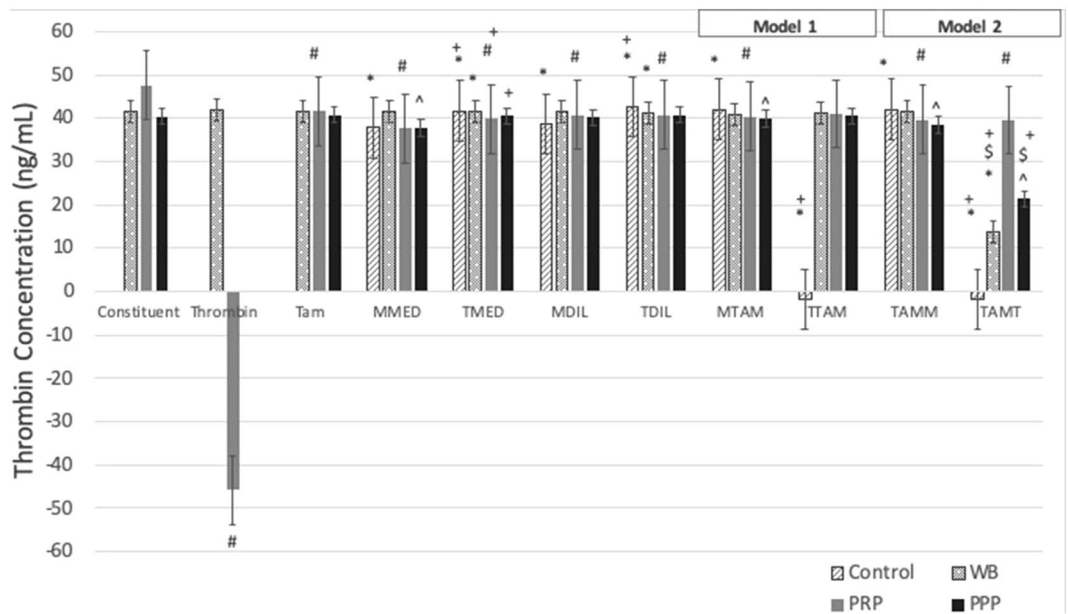


Figure 2. Bar graph showing thrombin generation in cumulative (Model 1) or circulatory (Model 2) Tamoxifen-therapy. Constituent: WB—untreated whole blood, PRP—untreated platelet-rich plasma, PPP—untreated platelet-poor plasma. Thrombin: Positive controls—WB and PRP incubated with 0.1 U/mL of thrombin. Tam: Tamoxifen-treatment of blood constituents (WB/PRP/PPP). Cells: M—MCF7 cells, T—T47D cells. M/TMED: conditioned media control of MCF7/T47D cells. M/TDIL: diluent control of MCF7/T47D cells. Model 1: M/T TAM: Tamoxifen-treated MCF7/T47D cells. Model 2: TAM M/T: Tamoxifen-treated blood constituents exposed to MCF7/T47D cells. * $p < 0.05$ compared to untreated WB; # $p < 0.05$ compared to untreated PRP; ^ $p < 0.05$ compared to untreated PPP. S $p < 0.05$ between matched cell lines compared between models.

($p < 0.05$) which was also visually evident (Figs. 3a-C, 4a-C). PRP exposed to T47D cells (Table 1) showed a decrease in CD62P IPA and an increase in CD63 IPA, with a slight shift to later stage activation, apparent in ultrastructural assessment (Fig. 4a-C), with WB exposure inducing lower levels of activation (Fig. 4a-A). While PPP exposure to T47D cells indicated the presence of fibrin, with some platelets still evident (Fig. 4a-E).

Effects of cumulative Tamoxifen (Model 1) on hypercoagulation. Cumulative effects of Tamoxifen were mimicked by pre-treating cancer cell lines (Model 1) prior to co-incubation with blood constituents. Tamoxifen-treated MCF7 breast cancer cells (Model 1) induced significantly greater secretion of thrombin ($p = 1.7E-06$) when compared to conditioned media from the untreated MCF7 cell line control (Fig. 2). This was reduced on exposure to all blood constituents, indicative of platelet activation, in WB (Fig. 5a-A) and PRP (Fig. 5a-C) samples, and fibrin formation in PPP (Fig. 5a-E). In WB exposed Tamoxifen-treated MCF7 cells, CD63 and CD62P IPA increased, the latter significantly compared to untreated WB and comparable to that of WB exposed to untreated MCF7 cells (Table 1). Moreover, platelet activation was in a later stage ($p > 0.05$) (Table 1), with corresponding morphology showing spreading of the hyalomere (Fig. 5a-A). This contrasted with PRP exposed to Tamoxifen-treated MCF7 cells where CD63 and CD62P IPA was lower compared to untreated PRP (Table 1) reflecting platelets at an earlier stage of activation with pseudopodia extension and the presence of microparticles and fibrin (Fig. 5a-C).

Tamoxifen-treated T47D cells significantly heightened levels of thrombin generation ($p = 1.30E-06$) much higher than the detectable levels of the assay itself, resulting in a negative value of $-1.83 \text{ ng/mL} \pm 2.78E+00$, as seen in the positive control PRP exposed to thrombin (Fig. 2). When compared to matched untreated T47D cells exposed to blood constituents; Tamoxifen pre-treatment of cells exposed to WB reduced thrombin detection (Fig. 2); however, early platelet activation was evident with a significant increase in CD62P IPA ($p = 0.046$) and CD63 IPA ($p = 0.04$) and corresponding extension of pseudopodia, spread of the hyalomere and microparticle release (Table 1, Fig. 6a-A). PRP exposure to Tamoxifen-treated T47D cells significantly increased thrombin generation (Fig. 2) and CD62P IPA and CD63 IPA (Table 1). Platelet activation indicated a shift to a later stage (Table 1); with platelets presenting spread hyalomeres, extending lamellipodia and filipodia, and early aggregation (Fig. 6a-C). Both PRP and PPP induced fibrin formation (Fig. 6a-C,E). The induction of hypercoagulation, was thus more evident by the T47D cell line.

Effects of circulating Tamoxifen (Model 2) on hypercoagulation. The effects of pre-treatment of whole blood with Tamoxifen (and subsequent separation into blood constituents) on coagulation was first assessed. Thrombin availability was significantly reduced only in PRP samples ($p = 1.17E-06$) (Fig. 2) and increased overall CD62P and CD63 IPA in WB ($p > 0.05$) and PRP ($p < 0.05$; $p = 0.03$), detected (Table 1). This

Marker of activation	Controls				Model 1				Model 2			
	WB	WBThr	WBTam	MMEDWB	TMEDWB	MDLWB	TDILWB	MTAMWB	TTAMWB	WBTAMM	WB TAMT	
Q2 (I1–I5)												
CD62P	3.93E+05 ± 1.72E+05	4.99E+05 ± 1.13E+05	4.93E+05 ± 2.07E+05	6.33E+05 ± 2.52E+05	4.31E+05 ± 1.73E+05	5.48E+05 ± 2.43E+05	3.63E+05 ± 1.99E+05	6.24E+05 ± 1.67E+05	7.78E+05* ± 3.96E+05	6.26E+05 ± 1.56E+05	6.01E+05* ± 2.37E+05	
CD63	2.92E+06 ± 8.06E+05	3.35E+06 ± 9.00E+05	3.01E+06 ± 1.58E+06	3.65E+06 ± 1.56E+06	4.08E+06 ± 1.35E+06	3.15E+06 ± 1.28E+06	2.80E+06 ± 1.97E+06	3.07E+06 ± 1.38E+06	4.87E+06 ± 2.36E+06	3.64E+06 ± 9.63E+05	3.69E+06 ± 1.68E+06	
Platelet Progression (CD62P/CD63)	1.35E-01 ± 0.016	1.49E-01 ± 0.013	1.64E-01 ± 0.026	1.74E-01 ± 0.019	1.06E-01 ± 0.019	1.74E-01 ± 0.020	1.30E-01 ± 0.015	2.03E-01 ± 0.026	1.60E-01 ± 0.022	1.72E-01 ± 0.019	1.63E-01 ± 0.036	
Controls												
PRP		PRPThr	PRPTam	MMEDPRP	TMEDPRP	MDILPRP	TDILPRP	MTAMPRP	TTAMPRP	PRPTAMM	PRPTAMT	
Q2 (I1–I5)												
CD62P	1.35E+06* ± 1.79E+05	7.60E+05 ± 1.44E+05	7.73E+05 ± 1.67E+05	1.20E+06 ± 5.24E+05	1.20E+06 ± 5.05E+05	7.07E+05 ± 4.72E+05	1.76E+06* ± 4.72E+05	8.62E+05 ± 6.04E+05	2.08E+06 ± 6.27E+05	7.16E+05 ± 2.73E+05	1.52E+06 ± 2.52E+05	
CD63	6.99E+06* ± 2.53E+06	8.41E+06 ± 1.35E+06	9.04E+06 ± 1.55E+06	1.25E+07* ± 3.80E+06	8.39E+06* ± 4.07E+06	7.93E+06 ± 3.57E+06	1.14E+07* ± 4.15E+06	6.11E+06 ± 4.66E+06	1.23E+07* ± 4.87E+06	7.92E+06 ± 2.28E+06	1.01E+07* ± 1.95E+06	
Platelet Progression (CD62P/CD63)	1.53E-01 ± 0.020	9.04E-02 ± 0.022	8.55E-02 ± 0.015	9.62E-02* ± 0.015	1.43E-01 ± 0.022	8.92E-02 ± 0.023	1.54E-01 ± 0.011	1.41E-01 ± 0.028	1.69E-01 ± 0.024	9.03E-02 ± 0.025	1.50E-01 ± 0.024	

Table 1. Index of platelet activation (IPA) for markers CD62P and CD63, and platelet progression (CD62P/CD63 ratio) in blood constituents; WB/PRP exposed to Tamoxifen-treated breast cancer cells (Model 1) and Tamoxifen-treated blood constituents; WB/PRP exposed to breast cancer cells (Model 2). Overall levels (Q2; I1–I5) were assessed. Bold p < 0.05 compared to untreated WB; *p < 0.05 compared to matched cell line exposed to WB (M/T MEDWB); italics p < 0.05 compared to matched cell lines between Models; underline p < 0.05 compared to untreated PRP; #p < 0.05 compared to matched cell line exposed to PRP (M/T MEDPRP); ± standard error of mean. WB untreated whole blood, WBThr positive control incubated with 0.1 U/ml thrombin, WBTam Tamoxifen-treated WB, Cells M—MCF7, T—T47D, Model 1: M/T MEDWB WB exposed to MCF7/T47D cells, M/T DILWB WB exposed to diluent-treated MCF7/T47D cells, M/T TAMWB WB exposed to Tamoxifen-treated MCF7/T47D cells, Model 2: WBTAM M/T Tamoxifen-treated WB exposed to MCF7/T47D cells.

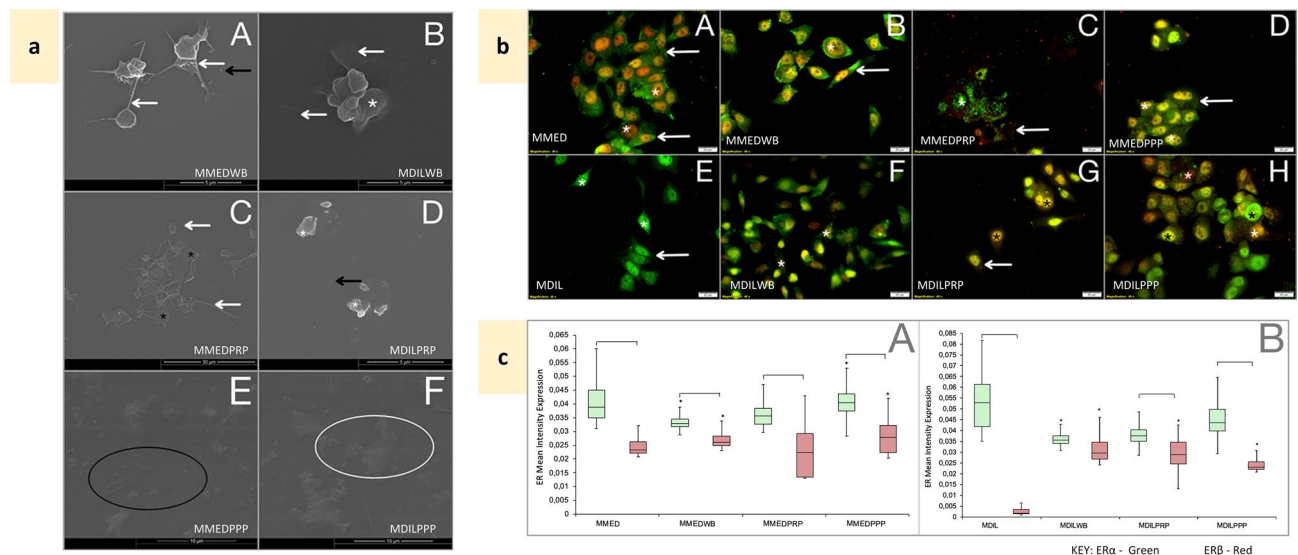


Figure 3. Effects of blood constituent incubation with MCF7 cells—controls. *MMED* media-treated MCF7 cells, *MMEDWB* WB co-incubated with media-treated MCF-7 cells, *MMEDPRP* PRP co-incubated with media-treated MCF-7 cells, *MMEDPPP* PPP co-incubated with media-treated MCF-7 cells, *MDIL* diluent-treated MCF7 cells, *MDILWB* WB co-incubated with diluent-treated MCF-7 cells, *MDILPRP* PRP co-incubated with diluent-treated MCF-7 cells, *MDILPPP* PPP co-incubated with diluent-treated MCF-7 cells. (a) Platelet ultrastructural alterations. White*—membrane folds, black*—hyalomere spread, white arrow—extending filipodia, black arrow—microparticles, white circle—fibrin, black circle—fibrin pores A: *MMEDWB*—active platelets, smooth membrane, extending filipodia and microparticles. B: *MDILWB*—platelets with membrane folds and filipodia. C: *MMEDPRP*—spread platelets and filopodia. D: *MDILPRP*—platelets with membrane folds and microparticles. E: *MMEDPPP* and F: *MDILPPP*—remnants of platelets, fibrin and pores. (b) Co-localisation of ERα (green) and ERβ (red) in MCF7 cells, following exposure to blood constituents. A: *MMED*—primarily cytoplasmic (white arrow) ERα and nuclear (*) ERβ expression. B: *MMEDWB*—cellular processes extend, cytoplasmic ERα and nuclear ERβ. C: *MMEDPRP*—diffuse ERα and ERβ expression. D: *MMEDPPP*—high cytoplasmic ERα expression and ERβ contained within the nucleus. E: *MDIL*—nuclear and cytoplasmic ERα, some nuclear ERβ. F: *MDILWB*—nuclear and cytoplasmic ERα, greater nuclear ERβ expression. G: *MDILPRP* and H: *MDILPPP*—high ERα and ERβ nuclear expression, minimal cytoplasmic expression. (c) Box and whisker plots representing quantitative analysis of ERα (green) and ERβ (red) expression in MCF7 cells, following exposure to blood constituents. A: Conditioned media-treated MCF7 cells. B: Diluent-treated MCF7 cells (0.1% DMSO). * $p < 0.05$ between ERα and ERβ within the treatment group. * $p < 0.05$ between matched ERs compared to untreated MCF7.

indicated that platelet activation remained within early stages in Tamoxifen-treated WB (Table 1) while derived PRP showed a shift to a later stage of platelet activation (Table 1) with platelets more active and aggregated than those from WB (Figs. 5a, 6a).

Tamoxifen pre-treated blood constituents were then exposed to untreated breast cancer cells to mimic circulating Tamoxifen (Model 2). When compared to Model 1, pre-treated WB exposed to untreated MCF7 cells induced a slightly higher level of thrombin generation (Fig. 2), with comparable levels of CD62P and CD63 IPA indicating early activation (Table 1, Fig. 5a–B). In Tamoxifen-treated PRP and PPP exposed to untreated MCF7 cells significantly lower thrombin was detected ($p = 1.30E-06$) (Fig. 2), reflecting binding and subsequent late stage platelet activation and aggregation in PRP (Table 1, Fig. 5a–D) and fibrin formation in PPP (Fig. 5a–F).

Thrombin activity in Tamoxifen-treated WB exposed to T47D cells was low; however, this is potentially due the binding of thrombin to the cells themselves (Fig. 6). Platelet activation was confirmed with both CD62P and CD63 IPA significantly heightened compared to untreated WB, similar to that of Model 1 (Table 1), with active platelets extending filipodia and fibrin deposits evident (Fig. 6a–B). Thrombin generation in Tamoxifen-treated PRP and PPP samples was also reduced compared to matched samples (Fig. 2). In PRP, this reflected corresponding low CD62P and CD63 IPA (Table 1), and platelet aggregation with platelets appearing exhausted (Fig. 6a–D). Notably in PPP, fibrinogen deposits reflected an inability of cells to mediate fibrin formation even though thrombin was present (Figs. 2, 6a–F).

ER expression in breast cancer cell lines alter under mediation by blood constituents. MCF7 cells typically have an epithelial-like morphology with thicker cellular processes (Fig. 3b–A). In untreated MCF7 cells, ERα (green fluorescence) is primarily cytoplasmic, with ERβ (red fluorescence) nuclear (Fig. 3b–A). Quantitative assessment showed overall, greater ERα expression than ERβ (Fig. 3c–A), even under exposure to blood constituents. On exposure to WB, ERα expression decreased ($p = 3.16E-50$) while ERβ increased ($p = 5.5E-20$) (Fig. 3b–B,c–A), significantly. A similar trend was observed under exposure to PRP; however, dispersed fluorescence was noted (Fig. 3b–C); but when exposed to PPP, both ERs increased significantly ($p = 4.08E-16$) (Fig. 3c–

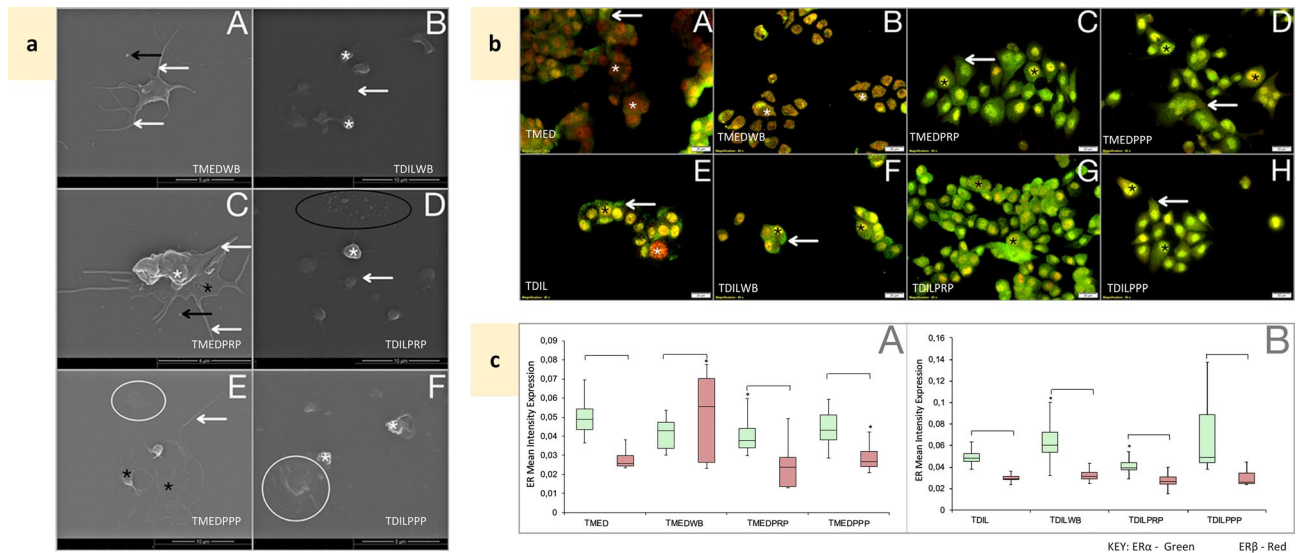


Figure 4. Effects of blood constituent incubation with T47D cells—controls. *TMED* media-treated T47D cells, *TMEDWB* WB co-incubated with media-treated T47D cells, *TMEDPRP* PRP co-incubated with media-treated T47D cells, *TMEDPPP* PPP co-incubated with media-treated T47D cells, *TDIL* diluent-treated T47D cells, *TDILWB* WB co-incubated with diluent-treated T47D cells, *TDILPRP*—PRP co-incubated with diluent-treated T47D cells, *TDILPPP* PPP co-incubated with diluent-treated T47D. (a) Platelet ultrastructural alterations. White *—membrane folds, black *—platelet hyalomere spread, white arrow—extending filipodia, black arrow—microparticles, white circle—fibrin, black circle—fibrin deposits. A: *TMEDWB*—slightly active platelet with filipodia and microparticles; B: *TDILWB*—mostly resting platelets; C: *TMEDPRP*—spread platelet, filipodia and microparticles. D: *TDILPRP*—platelets with smooth membrane and extending filipodia, with microparticles. E: *TMEDPPP*: fully spread platelets with fibrin deposits. F: *TDILPPP*: fibrin plaque formation. (b) Co-localisation of ER α (green) and ER β (red) in T47D cells, following exposure to blood constituents. A: *TMED*: primarily cytoplasmic ER α (white arrow) and ER β expression in the nucleus (*). B: *TMEDWB*: ER α and ER β expression in the nucleus (*). C: *TMEDPRP*: cytoplasmic and nuclear ER α expression (arrow) and nuclear ER β (*). D: *TMEDPPP*: high cytoplasmic ER α (white arrow) and nuclear ER β (*). E: *TDIL*—diffuse cytoplasmic and nuclear ER α (white arrow), nuclear ER β (*). F: *TDILWB*—cytoplasmic and nuclear ER α (white arrow), higher nuclear ER β (*). G: *TDILPRP*—cytoplasmic and nuclear ER α and nuclear ER β (*). H: *TDILPPP*—high nuclear and cytoplasmic ER α (black *) and higher nuclear ER β (white *). (c) Box and whisker plots representing quantitative analysis of ER α (green) and ER β (red) expression in T47D cells, following exposure to blood constituents. A: Conditioned media-treated T47D cells. B: Diluent-treated T47D cells (0.1% DMSO). *Significant differences between ER α and ER β within the treatment group. *Significant ($p < 0.05$) differences between matched ERs compared to untreated T47D.

A), with heightened ER α intensity in the nucleus (Fig. 3b-D). The diluent control showed similar expression profiles, with lower ER β (Fig. 3b-E–H,c-B).

T47D cells demonstrate a highly cohesive cobblestone appearance, with ER α similarly cytoplasmic and ER β mostly nuclear; however, ER β expression is consistently higher compared to that of MCF7 cells ($p > 0.05$) (Fig. 4b-A,c-A). Exposure to WB resulted in translocation of ER α to the nucleus (Fig. 4b-B), with variable and significantly higher ER β expression ($p = 7.04E-06$); similarly, PPP induced an increase in ER β albeit not as high (Fig. 4b-D). Levels of both markers were reduced on exposure to PRP (Fig. 4b-C). Notably, the diluent control showed some variation and as such is presented (Fig. 4b-E–H,c-B).

Tamoxifen alters ER expression in both models. In Model 1, in which blood constituents were co-cultured with Tamoxifen-treated MCF7 cells, ER α expression (primarily cytoplasmic) was consistently higher than ER β (primarily nuclear) (Fig. 5b-B–D,c) compared to Tamoxifen-treated MCF7 cells (Fig. 5b-A). However, Tamoxifen-treated whole blood exposed to untreated MCF7 cells (Model 2) (Fig. 5b-E), significantly heightened ER α and ER β expression (Fig. 5c), in the perinuclear and nuclear regions, respectively. This trend was similar to that induced by Tamoxifen-treated PPP (Fig. 5b-G). Conversely, Tamoxifen-treated PRP induced significantly reduced ER β ($p = 1.16E-21$), although considerable variation within the nucleus was noted (Fig. 5b-F,c).

Tamoxifen treatment induced higher ER α expression in T47D cells (Fig. 6b-A,c), similar to its effects on MCF7 cells (Fig. 5b-A,c). WB exposure to Tamoxifen pre-treated T47D cells (Model 1) increased ER α ($p = 1.48E-25$) and ER β ($p = 2.85E-42$) expression significantly (Fig. 6c), in the cytoplasm and nucleus respectively (Fig. 6b-B). PRP exposure caused translocation of ER α to the nucleus and ER β to the cytoplasm (Fig. 6b-C); however, mean intensity dropped significantly (Fig. 6c). PPP exposure followed a similar pattern (Fig. 6b-D,c). In Model 2, T47D cells exposed to Tamoxifen-treated WB significantly heightened nuclear ER β ($p = 1.38E-06$) expression and reduced ER α (although some cells show high intensity spots) (Fig. 6b-E), Tamoxifen-treated PPP followed

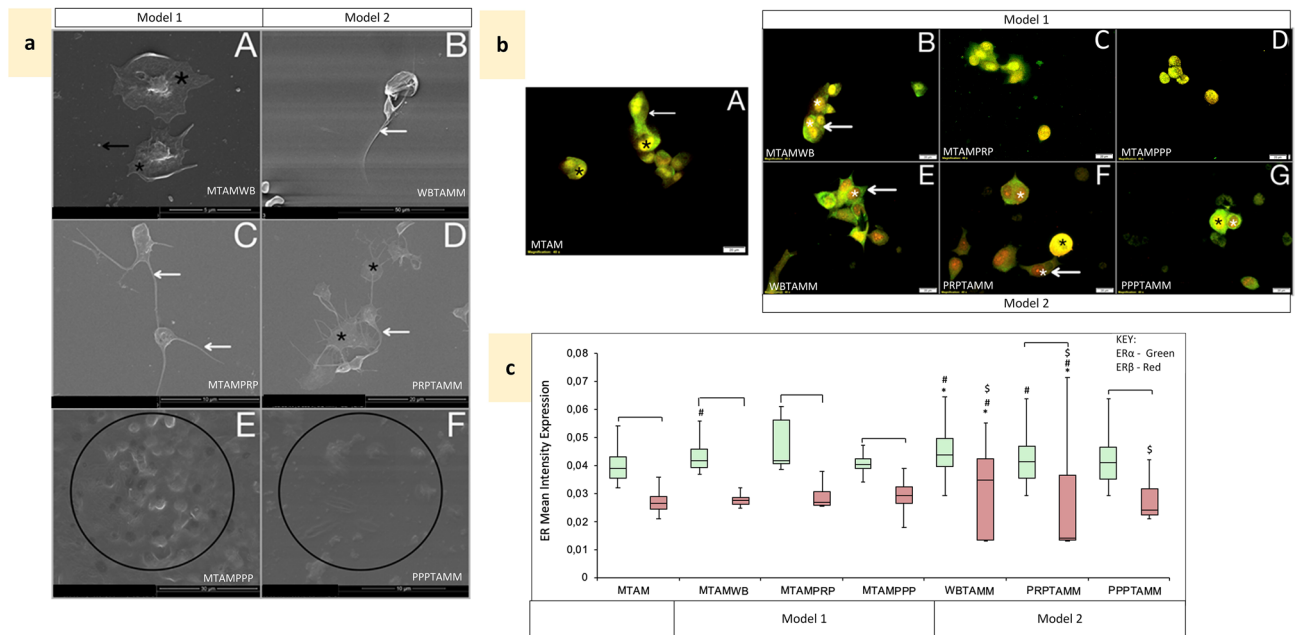


Figure 5. Effects of Tamoxifen treatment, cumulative (Model 1) and circulatory (Model 2) following co-incubation with MCF7 cells. *MTAM* Tamoxifen-treated MCF7 cells. *MTAMWB* Tamoxifen-treated MCF7 cells co-incubated with WB. *MTAMPRP* Tamoxifen-treated MCF7 cells co-incubated with PRP. *MTAMPPP* Tamoxifen-treated MCF7 cells co-incubated with PPP. *WBMTAM* Tamoxifen-treated WB co-incubated with MCF7 cells. *PRPTAMM* Tamoxifen-treated PRP co-incubated with MCF7 cells. *PPPTAMM* Tamoxifen-treated PPP co-incubated with MCF7 cells. (a) Platelet ultrastructural alterations. Black *—platelet hyalomere spread, white arrow—extending filipodia, black arrow—microparticles, black circle—fibrin clots and plaques with pores. A: *MTAMWB*—active platelets with a hyalomere spread and microparticles. B: *WBMTAM*—active platelets with a folded membrane and extending filipodia. C: *MTAMPRP*—platelets with a hyalomere spread and extending filipodia. D: *PRPTAMM*—platelets in early stages of aggregation, with extending filipodia. E: *MTAMPPP*—fibrin plaque formation with some pores. F: *PPPTAMM*—fibrin pores and remnants of fibrin. (b) Co-localisation of ERα (green) and ERβ (red) in MCF7 cells; following Tamoxifen-treatment and exposure to blood constituents (Model 1) and Tamoxifen-treatment of blood constituents exposed to MCF7 cells (Model 2). A: *MTAM*—cytoplasmic and nuclear ERα (arrow) and nuclear ERβ (*). B: *MTAMWB*—nuclear and cytoplasmic ERα (arrow) and nuclear ERβ (*). C: *MTAMPRP*—nuclear and low cytoplasmic ERα (arrow) and nuclear ERβ (*). D: *MTAMPPP*—low cytoplasmic and high nuclear ERα (arrow) and nuclear ERβ (*). E: *WBMTAM*—high cytoplasmic ERα (arrow) and extremely high nuclear ERβ (*). F: *PRPTAMM*—low cytoplasmic ERα (arrow) and high nuclear ERβ (white *), combined expression is noted (black *). G: *PPPTAMM*—cytoplasmic ERα with nuclear of ERβ (*). (c) Box and whisker plots representing quantitative analysis of ERα (green) and ERβ (red) expression in MCF7 cells for Model 1 and 2. [†] $p < 0.05$ between ERα and ERβ within the treatment group. [#] $p < 0.05$ between matched ERs compared to untreated MCF7. * $p < 0.05$ between matched ERs compared to Tamoxifen-treated MCF7. [§] $p < 0.05$ between matched ERs and blood constituent groups compared between models.

a similar trend (Fig. 6b–G,c). This contrasted with the effects of Tamoxifen-treated PRP where both ERs were reduced (Fig. 6b–F).

When assessing matched groups (Figs. 5c, 6c), overall the MCF7 cell line differentially responded to blood constituents, whereas the T47D cell line at least in Model 1, responded by primarily increasing ERβ expression.

Weak correlation between hypercoagulation and ER expression. Overall, significant ($p < 0.05$), positive ($r > 0.5$) correlation was found between CD62 and CD63 expression; while significant correlations were also found between ERβ, ERα and markers of platelet activation, they remained weak (Table 2).

Discussion

Modelling the clinical environment *ex vivo* allows investigation of cellular responses with reduced interference but is also limited by varying methodologies and approaches that may affect outcome. In the tumour microenvironment, platelets play a key role in priming tumour cells for metastasis, even before clinical diagnosis⁴⁶, and in the metastatic process itself^{25,26,28,29}. During this process, changes in coagulatory mechanisms may lead to thromboembolic complications³. Tamoxifen is known clinically, to increase risk of a thromboembolic event^{2,47}, but laboratory investigations provide contradictory results, most likely due to varying methodologies^{30,32,33}. Furthermore Tamoxifen is also used as a chemopreventive agent^{48,49}, and despite published clinical studies indicating its association with hypercoagulation^{7–9}, the risk of thrombosis is not readily considered in future clinical

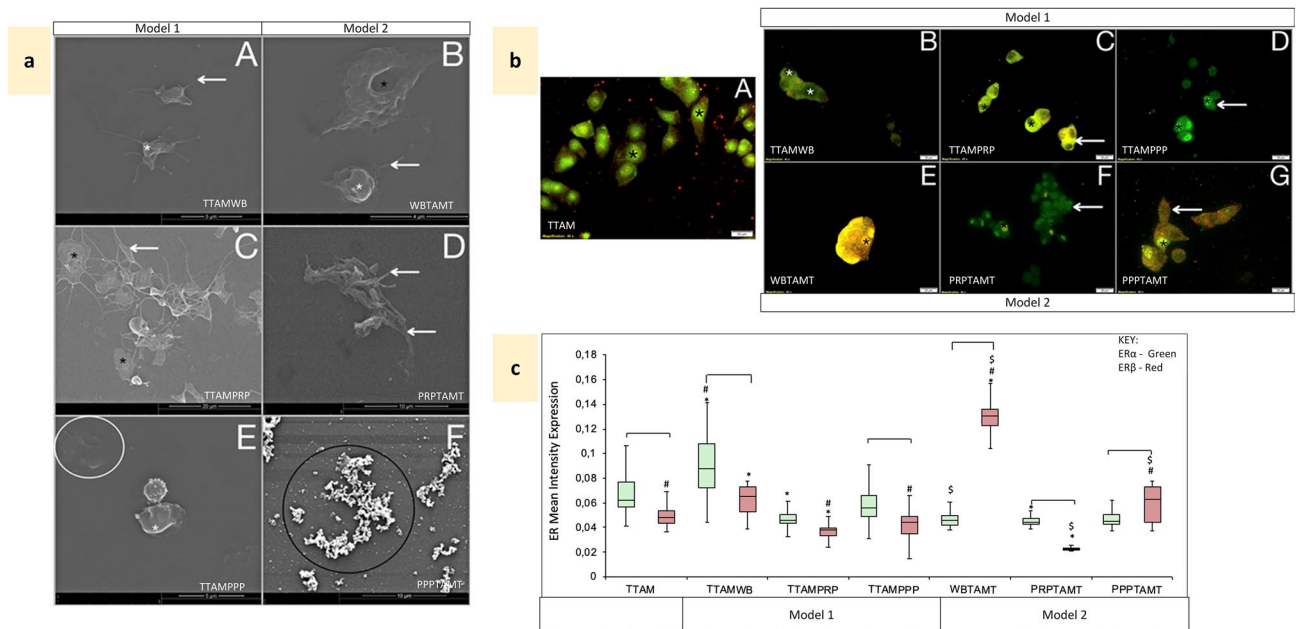


Figure 6. Effects of Tamoxifen treatment, cumulative (Model 1) and circulatory (Model 2) following co-incubation with T47D cells. *TTAM* Tamoxifen-treated T47D cells. *TTAMWB* Tamoxifen-treated T47D cells co-incubated with WB. *TTAMPRP* Tamoxifen-treated T47D cells co-incubated with PRP. *TTAMPPP* Tamoxifen-treated T47D cells co-incubated with PPP. *WBTAMT* Tamoxifen-treated WB co-incubated with T47D cells. *PRPTAMT* Tamoxifen-treated PRP co-incubated with T47D cells. *PPPTAMT* Tamoxifen-treated PPP co-incubated with T47D cells. **(a)** Platelet ultrastructural alterations. White *—membrane folds, black *—platelet hyalomere spread, white arrow—extending filipodia, black arrow—microparticles, white circle—fibrin, black circle—fibrin deposits. A: *TTAMWB*—active platelets with a folded membrane and extending filipodia. B: *WBTAMT*—active platelets with a folded membrane and extending filipodia with fibrin deposits and pores. C: *TTAMPRP*—platelets with a hyalomere spread and extending filipodia. D: *PRPTAMT*—platelets with extending filipodia. E: *TTAMPPP*—fibrin deposits and plaque formation with some pores. F: *PPPTAMT*—fibrinogen deposits. **(b)** Co-localisation of ER α (green) and ER β (red) in T47D cells; following Tamoxifen-treatment and exposure to blood constituents (Model 1) and Tamoxifen-treatment of blood constituents exposed to MCF7 cells (Model 2). A: *TTAM*—cytoplasmic and nuclear ER α (*) and ER β dispersed. B: *TTAMWB*—cytoplasmic ER α and nuclear ER β with some nuclei devoid of expression (*). C: *TTAMPRP*—low cytoplasmic ER α (arrow) and cytoplasmic ER β , with the nucleus devoid of expression (*). D: *TTAMPPP*—low cytoplasmic and high nuclear ER α (arrow) with nuclear ER β (*). E: *WBTAMT*—cytoplasmic ER α and extremely high nuclear ER β (*). F: *PRPTAMT*—low cytoplasmic ER α (arrow) with nuclear ER α and ER β (*). G: *PPPTAMT*—cytoplasmic and nuclear ER α (*), and cytoplasmic ER β (arrow). **(c)** Box and whisker plots representing quantitative analysis of ER α (green) and ER β (red) expression in T47D cells for Model 1 and 2. # $p < 0.05$ between ER α and ER β within the treatment group. * $p < 0.05$ between matched ERs compared to untreated T47D. $\dagger p < 0.05$ between matched ERs compared to Tamoxifen-treated T47D. $\S p < 0.05$ between matched ERs and blood constituent groups compared between models.

scenarios. We mimicked accumulation of Tamoxifen at the tumour site (Model 1), and recreated intravenously administered Tamoxifen (Model 2)⁵, in addition to testing blood constituents. In both models we identified that platelets in PRP were more active, shown morphologically and by expression of CD62P and CD63 markers, than those derived from whole blood. However, these platelets remained responsive due to PRP being generated by soft centrifugation⁵⁰. PRP did elicit more thrombin via granular release⁵¹, than WB, which compounded breast cancer-cell induced hypercoagulation.

A hypercoagulable state, also known as a prothrombotic state, in malignant cancers occurs when tumour cells activate the coagulation system and cause thrombi, formed by intravascular platelet aggregates^{52,53}. We show that breast cancer cell lines induce a hypercoagulatory environment mediated by secretion of thrombin, a procoagulant factor. Thrombin is not readily generated by the non-tumorigenic cell line, MCF10A, as shown by our results echoing other studies which also indicate that MCF10A express low to no PAR1 receptors^{54–56}. This suggests that the low levels of platelet activation and fibrin formation we identified were dependent on a different agonist, potentially Tissue Factor⁵⁷. We also found that on exposure to blood constituents, MCF10A cells alter ER α and ER β expression. Interestingly, studies suggest MCF10As present with a basal-like phenotype³⁵, capable of expressing luminal markers⁵⁵ or are undergoing epithelial-mesenchymal transition⁵⁸; thereby raising the question of whether these cells are an effective model of normal breast epithelial cells.

Expression of ER defines luminal phenotype cancers, which typically would be treated with hormone-therapy; pre-menopausal patients would undergo first-line treatment with Tamoxifen, regarded as the 'gold standard'^{59,60}. Studies suggest that hormone-therapies induce heightened sensitivity to thrombin by upregulating PAR receptors,

Spearman rank order correlations Highlighted correlations are significant at $p < 0.05$. $r = 0.6$																			
		Model 1						Model 2											
		Control			Thrombin generation			MCF7 Overall			T47D Overall								
	Overall	MMEDWB	MMEDPRP	TMEDWB	TMEDPRP	TMEDWB	TMEDPRP	MTAMWB	MTAMPRP	TAMWB	TAMPRP	TAMWB	TAMPRP	MCF7 Overall	T47D Overall	WBAMM	PRPTAMM	WBAMT	PRPTAMT
CD62P IPA	-0.075	-0.314	0.0857	-0.028	0.257	-0.242*	0.1319	-0.2	0.7714	0.3	0.3142	0.3	0.3142	-0.24795*	-0.06761	-0.6572	-0.486	-0.579	0.4
CD63 IPA	-0.047	-0.314	0.0285	0.314	0.428	-0.195	0.1018	-0.429	0.771	-0.7	-0.086	-0.7	-0.086	-0.17414	-0.03075	0.8986*	-0.4857	0.6	0.1
ER-Alpha	0.016	-0.714	0.0294	0.257	0.25	0.16584	0.0425	0.4857	-0.4857	0.3	0.1426	0.3	0.1426	0.173056	0.01357	0.3142	0.7714	-0.657	-0.1
ER-Beta	-0.189*	-0.2	-0.264	-0.257	0.142	-0.00069	-0.037	0.485	-0.1428	0.4	-0.314	0.4	-0.314	-0.2009	-0.10588	0.4286	-0.6	-0.486	-0.6

Table 2. Tabulation showing r values obtained from the nonparametric Spearman's correlation between CD62P, CD63 IPA and ER α and ER β , with thrombin detection for MCF7 and T47D cells. *MMEDWB* MCF7 cells exposed to WB, *MMEDPRP* MCF7 cells exposed to PRP, *MTAMWB* Tamoxifen-treated MCF7 cells exposed to WB, *MTAMPRP* Tamoxifen-treated MCF7 cells exposed to PRP, *WBAMM* MCF7 cells exposed to Tamoxifen-treated WB, *PRPTAMM* MCF7 cells exposed to Tamoxifen-treated PRP, *TMEDWB* T47D cells exposed to WB, *TMEDPRP* T47D cells exposed to PRP, *TTAMWB* Tamoxifen-treated T47D cells exposed to WB, *TTAMPRP* Tamoxifen-treated T47D cells exposed to PRP, *WBAMT* T47D cells exposed to Tamoxifen-treated WB, *PRPTAMT* T47D cells exposed to Tamoxifen-treated PRP. * $p < 0.05$ compared to thrombin detection, italics $p < 0.05$ compared to CD62P IPA, bold $p < 0.05$ compared to CD63 IPA.

further increasing thromboembolic risk^{61–63}. Our results indicate an increase in thrombin generation in breast cancer cells treated with Tamoxifen. Notably both cell lines are implicated in the secretion of Platelet Activating Factor (PAF) under thrombin stimulation, which in addition to mediating platelet aggregation, in an autocrine manner also enhances tumour progression^{64,65}; however, T47D cells appeared to induce a more hypercoagulatory environment than MCF7 cells. Tamoxifen-treated T47D cells induced later stages of platelet activation associated with a loss of CD62P IPA and persistence of CD63 IPA reflecting hypercoagulation in both PRP and WB, compared to MCF7 cells. During early platelet activation, platelets undergo morphological alterations extending pseudopodia and spreading the cell membrane, while simultaneously releasing granular content^{51,66}. CD62P is released from platelet α -granules and exposed on the plasma membrane; as activation progresses it is lost^{50,66}. CD63, which is involved in recruitment of other platelets is said to be released from δ granules and lysosomes in the later stages of activation^{51,67}; however, our results show that CD63 is expressed coupled with morphological and biochemical signs of early activation. Both activation markers, in addition to growth factors and agonists can also be released from platelets as microparticles^{68,69}, which we observed in ultrastructural analysis.

In Model 2, MCF7 cells induced a similar level of hypercoagulation in Tamoxifen-treated blood constituents as Model 1; however, T47D cells showed an even greater propensity to induce hypercoagulation, losing expression of both platelet activation markers possibly to their role in mediating platelet aggregation or shed as microparticles, and essentially ‘exhausting’ platelets⁷⁰. Notably, in platelet-poor plasma samples, fibrinogen deposits were readily available, indicating that the available thrombin, as opposed to facilitating fibrin formation as in MCF7 co-culture, may have rather competitively and selectively bound to PAR receptors which are reportedly more highly expressed on T47D cells than MCF7 cells^{71,72}.

To better understand why MCF7 and T47D cells induce hypercoagulation variably, we assessed their sub-phenotype using markers that have clinical relevance. In both cell lines ER α expression was typically higher than ER β expression, as expected. While the genomic actions of ER α are relatively well understood and the non-genomic actions of ER α less so⁶⁰, there remains considerable lack of clarity on the role of ER β in breast tumour progression. High ER β expression has been implicated in breast tumour development, and notably in Tamoxifen-resistance⁶⁰; however, more studies indicate that it may be associated with a more favourable response to treatment^{73,74}, and that its reduction is associated with the transition to a more invasive phenotype⁶⁰. Interestingly, T47D cells which are regarded as more invasive than MCF7 cells by expressing more proteins associated with tumorigenesis, growth and prevention of apoptosis⁷⁵, presented with higher standard ER β expression than MCF7 cells. Hormone-dependent tumours are identified by ER α overexpression, and while Tamoxifen mediates ER activity, downregulation of the receptor is associated with the transition to a more aggressive phenotype that does not respond to therapy, a common evasive strategy employed by tumour cells⁶⁰. We identified that in both cell lines, exposure to WB resulted in a significant increase in ER β expression; while in T47D cells, translocation of ER α to the nucleus may reflect engagement of genomic activities⁶⁰. Recall that for this study, blood was collected from volunteers between days 1 and 10 of the menstrual cycle due to the lower levels of oestrogen and progesterone present⁷⁶, with the aim of limiting the action of these hormones. Nevertheless, in both cell lines, and both models there was considerable variation induced by blood components; while MCF7 cells responded differentially, T47D cells demonstrated more of a pattern dominated by heightened ER β . Furthermore, in Model 2 T47D cells specifically showed a reduction in ER α expression when compared to Model 1, indicating the efficacy of circulating Tamoxifen to not only heighten ER β but downregulate ER α for a positive outcome. While WB better replicates the concept of circulatory interaction with tumour cells, many studies employ PRP to ascertain specific effects induced by platelets. However, we show that ER expression is sensitive to such conditions and postulate that the variation seen in our study is due to the generation of PRP, which even with soft centrifugation, provides a more concentrated source of growth factors⁷⁷. This is notwithstanding that platelets themselves express ER^{78,79}, possibly explaining the ‘exhaustion’ seen under direct Tamoxifen treatment; even PPP contains high concentrations of microparticles which contain a further host of growth factors, albeit at lesser levels⁸⁰.

ER positive breast tumours are associated with tailored therapeutic approaches^{81,82}, which increase the risk for thromboembolic complications. Our results highlight the procoagulant nature of breast cancer cells themselves and substantiate clinical studies indicating that Tamoxifen, regardless of model used, induces a hypercoagulatory environment, mediated by platelet interaction with tumour cells. The crucial role that platelets play in the tumour microenvironment is thus mediated by a host of secreted factors enabling cross-talk with tumour cells. Notably, changes in cytosolic and membrane ER α is postulated to relate to alterations of the metastatic potential of breast cancer cells, in which prothrombotic cytokines and thrombin⁸³ are released to induce a hypercoagulable state to facilitate tumour progression^{21,29,68,84}. This relationship is highlighted by the weak, yet positive correlation we identified between ERs, and the CD62P and CD63 IPA; indicating an association between tumour invasion profiles and hypercoagulation, however, it is noted that in addition to ER expression, other yet unknown factors may play a predictive role in defining hypercoagulation.

Materials and methods

Human Research Ethics Clearance was obtained from the Human Ethics Research Committee (Medical), University of the Witwatersrand, Clearance Certificate Number M160826. Informed consent was obtained from all participants and all research was performed in accordance with the ethical guidelines.

Cell culture. MCF7 cells and T47D cells obtained from the American Type Culture Collection (ATCC) were cultured as follows: MCF7 cells (P36) in DMEM (Dulbecco’s Modified Eagles Medium), with 10% FBS (Foetal Bovine Serum), 0.1% P/S (Penicillin/Streptomycin); T47D cells (P29) in RPMI (Roswell Park Memorial Institute Medium) with 0.2 U/mL bovine insulin, 10% FBS and 0.1% P/S. MCF10A, a non-tumorigenic breast epithelial

cell line, kindly donated by Prof Raquel Duarte was propagated in MEGM (Mammary epithelial cell growth medium BulletKit), supplemented with 100 ng/mL cholera toxin (Merck, Johannesburg, South Africa; C8052).

For experimentation, cells were seeded at 1×10^5 cells onto glass coverslips in a 24-well plate. MCF10A and MCF7 cells were seeded directly onto the glass whereas T47D cells were seeded onto glass coverslips coated with 5 mg/mL poly-D-lysine (Sigma-Aldrich; P6407) to facilitate attachment.

Whole blood acquisition. Peripheral whole blood (WB) was obtained from healthy female donors ($n=6$) between 19 and 30 years old into 3.2% sodium citrate vacuette coagulation tubes. The first 2 mL of blood drawn was discarded to exclude the effect of mechanically activated platelets⁸⁵. Participant exclusion criteria included pregnancy, contraceptive use, previously identified autoimmune diseases or immunodeficiency, previous history of cancer, cancer, smoking, and consumption of anti-platelet and/or anti-coagulation medication in the previous 72 h. Blood was collected between days 1 and 10 of the menstrual cycle due to the lower levels of oestrogen and progesterone present within the circulating blood⁷⁶.

Establishment of Model 1 and Model 2 co-culture systems. For Model 1: Samples of WB were centrifuged at $200\times g$ to yield platelet-rich plasma (PRP), and at $400\times g$ to yield platelet-poor plasma (PPP). MCF7 and T47D cells were pre-treated with 2 μM Tamoxifen³⁰ for 24 h prior to exposure to 200 μL WB, PRP or PPP for 2.5 min at room temperature (RT).

For Model 2: First WB was treated with 2 μM Tamoxifen for 1 h at RT. Subsequently, WB was centrifuged to yield PRP and PPP. Untreated MCF7 and T47D cells were then incubated with 200 μL Tamoxifen-treated WB, PRP or PPP for 2.5 min⁵⁰ at RT (Supplementary Fig. S1).

Appropriate controls including diluent [0.1% DMSO (Dimethyl Sulfoxide)], untreated blood constituents and untreated cells were prepared for all experiments. Positive controls for accurate assessment of platelet activation were prepared by incubating lysed WB or PRP with 0.1 U/mL of human thrombin- α (SANBS, South Africa), a platelet agonist, for 5 min⁵⁰.

Sample preparation for thrombin activity assay. The release of thrombin was tested using a Thrombin Activity Assay Kit (Abcam; ab 197006). Following co-culture, blood samples or supernatant as required were aspirated, snap-frozen in liquid nitrogen and kept at -80°C . For the assay, samples were thawed on ice and diluted at 1/10 with assay buffer. 6 standards were prepared to achieve thrombin concentrations of; 0 ng/well, 5 ng/well, 10 ng/well, 15 ng/well, 20 ng/well, 25 ng/well. Diluted samples were added to their respective wells at 50 μL . Both standard and sample wells were incubated with thrombin substrate diluted in assay buffer. Fluorescence was measured at Ex/Em = 350/450 using a GloMax Promega Plate Reader in a kinetic mode every 2 min for 60 min at 37°C , Department of Molecular Medicine and Haematology, University of the Witwatersrand.

Sample preparation for flow cytometry. Lysed WB and PRP samples were resuspended in 150 μL Tyrode's buffer. Samples were labelled with APC-conjugated mouse anti-human CD41a (BD Pharmingen; 559777), FITC-conjugated mouse anti-human CD62P (BD Pharmingen; 555523) and PE-Cy7 mouse anti-human CD63 (BD Pharmingen; 353010) at a concentration of 1:20 as determined using titration. Following compensation, experiments were conducted on an LSR Fortessa Flow Cytometer (BD Biosciences, South Africa). Events were recorded at 100,000 events per sample using FACSDiva Software (version 6.2) (BD Biosciences)⁸⁶. The platelet population was initially gated using a forward scatter (FSC) voltage of 300 V and a side scatter (SSC) voltage of 275 V followed by gating a singlet population using FSC-height and FSC-area. The parent platelet population was identified and further gated based on expression of the CD41a (APC, 565 V), CD62P (FITC, 469 V) and CD63 (PE-CY7, 645 V). Interval gates^{30,50} were drawn to classify a graded level of each platelet activation marker determined using Geometric Mean Fluorescence Intensity (gMFI) of the platelet population (Fig. 2). Data acquired was exported into Microsoft Excel.

Sample preparation for scanning electron microscopy. For both Models, WB samples underwent erythrocyte lysis using ammonium chloride buffer for 10 min at RT. Samples were centrifuged at $200\times g$ for 5 min and the supernatant discarded. The pellet was resuspended in 150 μL Tyrode's buffer. Thereafter, 20 μL each of; lysed WB, PRP or PPP were placed on glass coverslips in 24 well plates and incubated at 37°C in 5% CO_2 for 5 min for adhesion. Samples were washed in 0.1 M PBS on a microplate shaker for 20 min and fixed in 2.5% formaldehyde/glutaraldehyde for 15 min followed by rinsing thrice with 0.1 M PBS and secondary fixation in 1% osmium tetroxide. Following further rinsing in PBS, cells were dehydrated through an increasing series of ethanol (30%, 50%, 70%, 90%, and three times absolute ethanol), and dried using hexamethyldisilazane (HMDS). Samples were mounted onto aluminium stubs, coated by carbon evaporation and qualitative assessed using a FEI Nova 600 Scanning Electron Microscope with acceleration voltage set at 30 kV.

Sample preparation for immunolocalisation of ER α and ER β protein expression in breast cancer cells. MCF7 and T47D cells were washed thrice with 1 M PBS, fixed in 4% paraformaldehyde for 10 min at RT and washed with 0.1% Tween20/PBS. Cells were then incubated with 0.2% Triton X-100/PBS for 10 min at RT, washed three times with 0.1% Tween20/PBS for 5 min each and incubated in 1% BSA (Bovine Serum Albumin) in 0.1% Tween20/PBS for 30 min at RT. Cells were then incubated with Goat Anti-ER β (Abcam, ab288) and Rabbit Anti-oestrogen Receptor ER α (Abcam, ab32063) primary antibodies, at concentrations 1:400 and 1:200 in 0.1% Tween20/PBS, respectively (concentrations were determined by conducting a dilution assay), at 4°C overnight. Cells were then washed thrice with 0.1% Tween20/PBS and incubated with secondary antibodies

Alexa Fluor 488 anti-rabbit (Life Technologies, Johannesburg, South Africa, A11008) and Alexa Fluor 594 anti-goat (Life Technologies, A11005), at 1:1000 respectively, for 2 h at RT in the dark. Cells were again washed thrice with 0.1% Tween20/PBS and nuclei were counterstained with DAPI. After a final wash with 0.1% Tween20/PBS coverslips were mounted onto slides using Fluoromount (Sigma-Aldrich, F4680). Standard immunocytochemical technical controls were included.

Photomicrographs were obtained using an Olympus iX51 Inverted Fluorescent Microscope with cellSens Dimension Software (version 1.11)⁸⁷, School of Anatomical Sciences, University of the Witwatersrand. Photomicrographs were taken using filters: U-MNU2 to detect fluorescence from DAPI staining, U-MWIBA3 to detect cells stained with and expressing (ER α) Alexa Fluor 488 and U-MWIY2 to detect cells stained with and expressing (ER β) Alexa Fluor 594. Photomicrographs were obtained in grayscale at 40 \times magnification and quantitatively analysed using CellProfiler software (version 3.1.5)⁸⁸. In brief, DAPI photomicrographs were first processed to identify nuclei between a range between 40 and 100 pixels in diameter. Pixels that did not fall in this range or were on the boundary were discarded. The Background method was used for intensity thresholding and weighted variance was minimized with a non-adjusted “Threshold correction factor” indicated as 1. The lower bound was indicated at 0 and the upper bound was indicated at 1. Objects that were clumped were distinguished and separated using the “Intensity” method. Thereafter photomicrographs for Alexa Fluor 488 (ER α) were processed as ‘primary objects’. The Background method was used for intensity thresholding, again and weighted variance was minimized with a “Threshold correction factor” of 0.99. This was followed similarly, by identification of Alexa Fluor 594 (ER β) in the corresponding photomicrograph. Images were further processed to obtain data on colocalization, cell size, shape and mean intensity of ER α and ER β and exported to Microsoft Excel.

Data analysis. For flow cytometry, the index of platelet activation (IPA) was calculated for Q2 or each interval (I1-5) such that:

$$\text{IPA}^{\text{CD62P}} = \text{gMFI}(\text{CD62P}^+) \times \text{n}(\text{CD41}^+ \text{CD62P}^+ \text{ events}) \text{ or } \text{IPA}^{\text{CD63}} = \text{gMFI}(\text{CD63}^+) \times \text{n}(\text{CD41}^+ \text{CD63}^+ \text{ events})$$

All data from Microsoft Excel was then exported into Statistica Version 23 for analysis.

A Shapiro–Wilk test of normality determined that the data was not normally distributed. Moreover, to account for the limited sample size, non-parametric tests were used. The non-parametric Friedman test followed by a post-hoc Wilcoxon Matched Paired test, based on the dependency of blood constituents, was conducted to determine whether IPA, or thrombin availability or generation, or ER expression altered in response to hormone-therapy and blood constituent co-incubation. All tests were conducted at a confidence interval of 95%, and a significance level of 0.05.

Data availability

The Authors will make datasets available on request subject to requirements from the Human Research Ethics Committee, University of the Witwatersrand.

Received: 8 January 2020; Accepted: 23 September 2020

Published online: 06 November 2020

References

- Bray, F. *et al.* Global cancer statistics 2018: GLOBOCAN estimates of incidence and mortality worldwide for 36 cancers in 185 countries. *CA. Cancer J. Clin.* **68**, 394–424 (2018).
- Walker, A. *et al.* When are breast cancer patients at highest risk of venous thromboembolism? A cohort study using English health care data. *Blood* **127**, 849–858 (2017).
- Rugo, H. S. Dosing and safety implications for oncologists when administering everolimus to patients with hormone receptor-positive breast cancer. *Clin. Breast Cancer* **16**, 18–22 (2016).
- Masoud, V. & Pagès, G. Targeted therapies in breast cancer: New challenges to fight against resistance. *World J. Clin. Oncol.* **8**, 120–134 (2017).
- Ishitobi, M., Shibuya, K., Komoike, Y., Koyama, H. & Inaji, H. Preferences for oral versus intravenous adjuvant chemotherapy among early breast cancer patients. *Patient Prefer. Adherence* **7**, 1201–1206 (2013).
- Lin, H. F. *et al.* Correlation of the tamoxifen use with the increased risk of deep vein thrombosis and pulmonary embolism in elderly women with breast cancer: The case–control study. *Medicine (United States)* **97**, 20 (2018).
- Onitilo, A. A. *et al.* Clustering of venous thrombosis events at the start of tamoxifen therapy in breast cancer: A population-based experience. *Thromb. Res.* **130**, 27–31 (2012).
- Meier, C. R. & Jick, H. Tamoxifen and risk of idiopathic venous thromboembolism. *Br. J. Clin. Pharmacol.* **45**, 608–612 (1998).
- Walker, A. J. *et al.* CME Article When are breast cancer patients at highest risk of venous thromboembolism? A cohort study using English health care data. *Blood* **127**, 849–858 (2017).
- Decensi, A. *et al.* Effect of tamoxifen on venous thromboembolic events in a breast cancer prevention trial. *Circulation* **111**, 650–656 (2005).
- Jonat, W. *et al.* Effectiveness of switching from adjuvant tamoxifen to anastrozole in postmenopausal women with hormone-sensitive early-stage breast cancer: A meta-analysis. *Lancet. Oncol.* **7**, 991–996 (2006).
- Kmieciak, M. *et al.* Tumor escape and progression of HER-2/neu negative breast cancer under immune pressure. *J. Transl. Med.* **9**, 35 (2011).
- Mittendorf, E. A. *et al.* The neo-bioscore update for staging breast cancer treated with neoadjuvant chemotherapy. *JAMA Oncol.* **2**, 929 (2016).
- Howell, A. *et al.* Results of the ATAC (Arimidex, Tamoxifen, Alone or in Combination) trial after completion of 5 years’ adjuvant treatment for breast cancer. *Lancet* **365**, 60–62 (2005).
- Kim, Y., Kim, O. J. & Kim, J. Cerebral venous thrombosis in a breast cancer patient taking tamoxifen: Report of a case. *Int. J. Surg. Case Rep.* **6**, 77–80 (2015).
- Elaskalani, O., Berndt, M. C., Falasca, M. & Metharom, P. Targeting platelets for the treatment of cancer. *Cancers (Basel)* **9**, 20 (2017).

17. Eroglu, A. Tamoxifen-associated thromboembolism in breast cancer. *Thromb. Res.* **131**, 566 (2013).
18. Kovac, M. *et al.* Factor V Leiden mutation and high FVIII are associated with an increased risk of VTE in women with breast cancer during adjuvant tamoxifen—results from a prospective, single center, case control study. *Eur. J. Intern. Med.* **26**, 63–67 (2015).
19. Jayachandran, M. & Miller, V. M. Human platelets contain estrogen receptor alpha, caveolin-1 and estrogen receptor associated proteins. *Platelets* **14**, 75–81 (2003).
20. Dupuis, M. *et al.* Effects of estrogens on platelets and megakaryocytes. *Int. J. Mol. Sci.* **20**, 20 (2019).
21. Falanga, A., Russo, L. & Verzeroli, C. Mechanisms of thrombosis in cancer. *Thromb. Res.* **131**, S59–S62 (2013).
22. Mitrugno, A., Williams, D., Kerrigan, S. W. & Moran, N. A novel and essential role for Fc RIIa in cancer cell-induced platelet activation. *Blood* **123**, 249–260 (2014).
23. Nash, G. F., Turner, L. F., Scully, M. F. & Kakkar, A. K. Platelets and cancer. *Lancet Oncol.* **3**, 425–430 (2002).
24. Kreutz, R. P. *et al.* Protease activated receptor-1 (PAR-1) mediated platelet aggregation is dependant on clopidogrel response. *Thromb. Res.* **130**, 198–202 (2012).
25. Schlesinger, M. Role of platelets and platelet receptors in cancer metastasis. *J. Hematol. Oncol.* **11**, 125 (2018).
26. Li, R. *et al.* Presence of intratumoral platelets is associated with tumor vessel structure and metastasis. *BMC Cancer* **14**, 167 (2014).
27. Qi, C. *et al.* P-selectin-mediated platelet adhesion promotes tumor growth. *Oncotarget* **6**, 6584–6596 (2015).
28. Michael, J. V. *et al.* Platelet microparticles infiltrating solid tumors transfer miRNAs that suppress tumor growth. *Blood* **130**, 567–580 (2017).
29. Mezouar, S. *et al.* Role of platelets in cancer and cancer-associated thrombosis: Experimental and clinical evidences. *Thromb. Res.* **139**, 65–76 (2016).
30. Pather, K., Dix-Peek, T., Duarte, R., Chetty, N. & Augustine, T. N. Breast cancer cell-induced platelet activation is compounded by tamoxifen and anastrozole in vitro. *Thromb. Res.* **177**, 51–58 (2019).
31. Hernandez, R. K., Sørensen, H. T., Pedersen, L., Jacobsen, J. & Lash, T. L. Tamoxifen treatment and risk of deep venous thrombosis and pulmonary embolism. *Cancer* **115**, 4442–4449 (2009).
32. Johnson, K. E. *et al.* Tamoxifen directly inhibits platelet angiogenic potential and platelet-mediated metastasis highlights. *Arterioscler. Thromb. Vasc. Biol.* **37**, 664–674 (2017).
33. Chang, Y. *et al.* A novel role for tamoxifen in the inhibition of human platelets. *Transl. Res.* **157**, 81–91 (2011).
34. Sobczynski, D. J. *et al.* Drug carrier interaction with blood: A critical aspect for high-efficient vascular-targeted drug delivery systems. *Ther. Deliv.* **6**, 915–934 (2015).
35. Neve, R. M. *et al.* A collection of breast cancer cell lines for the study of functionally distinct cancer subtypes. *Cancer Cell* **10**, 515–527 (2006).
36. Holliday, D. L. & Speirs, V. Choosing the right cell line for breast cancer research. *Breast Cancer Res.* **13**, 215 (2011).
37. Ali, S. & Coombes, R. C. Estrogen receptor alpha in human breast cancer: Occurrence and significance. *J. Mammary Gland Biol. Neoplasia* **5**, 271–281 (2000).
38. Phung, M. T., Tin Tin, S. & Elwood, J. M. Prognostic models for breast cancer: A systematic review. *BMC Cancer* **19**, 230 (2019).
39. Bahreini, A. *et al.* Mutation site and context dependent effects of ESR1 mutation in genome-edited breast cancer cell models. *Breast Cancer Res.* **19**, 60 (2017).
40. Clatot, F., Augusto, L. & Di Fiore, F. ESR1 mutations in breast cancer. *Aging (Albany, NY)* **9**, 3–4 (2017).
41. Esslimani-Sahla, M. *et al.* Estrogen receptor (ER) level but not its ER cx variant helps to predict tamoxifen resistance in breast cancer. *Clin. Cancer Res.* **10**, 5769–5776 (2004).
42. Honma, N. *et al.* Clinical importance of estrogen receptor- β evaluation in breast cancer patients treated with adjuvant tamoxifen therapy. *J. Clin. Oncol.* **26**, 3727–3734 (2008).
43. Hopp, T. A. *et al.* Low levels of estrogen receptor protein predict resistance to tamoxifen therapy in breast cancer. *Clin. Cancer Res.* **10**, 7490–7499 (2004).
44. Weibrich, G., Hansen, T., Kleis, W., Buch, R. & Hitzler, W. Effect of platelet concentration in platelet-rich plasma on peri-implant bone regeneration. *Bone* **34**, 665–671 (2004).
45. Everts, P. A. M. *et al.* Platelet-rich plasma and platelet gel: A review. *J. Extra. Corpor. Technol.* **38**, 174–187 (2006).
46. Massagué, J. & Obenauf, A. C. Metastatic colonization by circulating tumour cells. *Nature* **529**, 298–306 (2016).
47. Fabian, C. J. The what, why and how of aromatase inhibitors: Hormonal agents for treatment and prevention of breast cancer. *Int. J. Clin. Pract.* **61**, 2051–2063 (2007).
48. Waters, E. A., McNeel, T. S., Stevens, W. M. & Freedman, A. N. Use of tamoxifen and raloxifene for breast cancer chemoprevention in 2010. *Breast Cancer Res. Treat.* **134**, 875–880 (2012).
49. Chang, M. Tamoxifen resistance in breast cancer. *Biomol. Ther.* **20**, 256–267 (2012).
50. Augustine, T. N., van der Spuy, W. J., Kaberry, L. L. & Shayi, M. Thrombin-mediated platelet activation of lysed whole blood and platelet-rich plasma: A comparison between platelet activation markers and ultrastructural alterations. *Microsc. Microanal.* **20**, 20 (2016).
51. Haemmerle, M., Stone, R. L., Menter, D. G., Afshar-Kharghan, V. & Sood, A. K. The platelet lifeline to cancer: Challenges and opportunities. *Cancer Cell* **33**, 965–983 (2018).
52. Caine, G. J., Stonelake, P. S., Lip, G. Y. H. & Kehoe, S. T. The hypercoagulable state of malignancy: Pathogenesis and current debate. *Neoplasia* **4**, 465–473 (2002).
53. Bauer, K. Risk and prevention of venous thromboembolism in adults with cancer—UpToDate. *UpToDate* (2019). <https://www.uptodate.com/contents/risk-and-prevention-of-venous-thromboembolism-in-adults-with-cancer>.
54. Booden, M. A., Eckert, L. B., Der, C. J. & Trejo, J. Persistent signaling by dysregulated thrombin receptor trafficking promotes breast carcinoma cell invasion. *Mol. Cell. Biol.* **24**, 1990–1999 (2004).
55. Qu, Y. *et al.* Evaluation of MCF10A as a reliable model for normal human mammary epithelial cells. *PLoS One* **10**, e0131285 (2015).
56. Reddel, C., Tan, C. & Chen, V. Thrombin generation and cancer: Contributors and consequences. *Cancers (Basel)* **11**, 100 (2019).
57. Berny-Lang, M. A. *et al.* Promotion of experimental thrombus formation by the procoagulant activity of breast cancer cells. *Phys. Biol.* **8**, 015014 (2011).
58. Sarrío, D., Mari, S., Hardisson, D., Cano, A. & Moreno-bueno, G. Epithelial–mesenchymal transition in breast cancer relates to the basal-like phenotype. *Cancer Res.* **20**, 989–997. <https://doi.org/10.1158/0008-5472.CAN-07-2017> (2008).
59. Zhai, G. *et al.* Diffusion weighted imaging evaluated the early therapy effect of tamoxifen in an MNU-induced mammary cancer rat model. *PLoS One* **8**, e6444 (2013).
60. Begam, A. J., Jubie, S. & Nanjan, M. J. Bioorganic chemistry estrogen receptor agonists/antagonists in breast cancer therapy: A critical review. *Bioorg. Chem.* **71**, 257–274 (2017).
61. Herkert, O., Kuhl, H., Sandow, J., Busse, R. & Schini-Kerth, V. B. Sex steroids used in hormonal treatment increase vascular procoagulant activity by inducing thrombin receptor (PAR-1) expression. *Circulation* **104**, 2826–2831 (2001).
62. Nag, J. & Bar-Shavit, R. Transcriptional landscape of PARs in epithelial malignancies. *Int. J. Mol. Sci.* **19**, 3451 (2018).
63. Jick, H., Kaye, J. A., Vasilakis-Scaramozza, C. & Jick, S. S. Risk of venous thromboembolism among users of third generation oral contraceptives compared with users of oral contraceptives with levonorgestrel before and after 1995: Cohort and case–control analysis. *BMJ* **321**, 1190–1195 (2000).
64. da Silva Junior, I. A., de Sousa Andrade, L. N., Jancar, S. & Chammass, R. Platelet activating factor receptor antagonists improve the efficacy of experimental chemo- and radiotherapy. *Clinics* **73**, e792s (2018).

65. Bussolati, B. *et al.* PAF produced by human breast cancer cells promotes migration and proliferation of tumor cells and neo-angiogenesis. *Am. J. Pathol.* **157**, 1713 (2000).
66. Smith, C. W. *et al.* TREM-like transcript 1: A more sensitive marker of platelet activation than P-selectin in humans and mice. *Blood Adv.* **2**, 2072–2078 (2018).
67. Baaten, C. C. F. M. J., ten Cate, H., van der Meijden, P. E. J. & Heemskerk, J. W. M. Platelet populations and priming in hematological diseases. *Blood Rev.* **31**, 389–399 (2017).
68. Zhang, N. & Newman, P. J. Packaging functionally important plasma proteins into the α -granules of human-induced pluripotent stem cell-derived megakaryocytes. *J. Tissue Eng. Regen. Med.* **13**, 244–252 (2019).
69. Plantureux, L., Crescence, L., Dignat-George, F., Panicot-Dubois, L. & Dubois, C. Effects of platelets on cancer progression. *Thromb. Res.* **164**, S40–S47 (2018).
70. van der Zee, P. M. *et al.* P-selectin- and CD63-exposing platelet microparticles reflect platelet activation in peripheral arterial disease and myocardial infarction. *Clin. Chem.* **52**, 657–664 (2006).
71. Diaz, J. *et al.* Progesterone promotes focal adhesion formation and migration in breast cancer cells through induction of protease-activated receptor-1. *J. Endocrinol.* **214**, 165–175 (2012).
72. Kamath, L., Meydani, A. & Foss, F. Signaling from protease-activated receptor-1 inhibits migration and invasion of breast cancer cells. *Cancer Res.* **61**, 5933–5940 (2001).
73. Omoto, Y., Eguchi, H., Yamamoto-Yamaguchi, Y. & Hayashi, S. Estrogen receptor (ER) beta1 and ERbeta2 inhibit ERalpha function differently in breast cancer cell line MCF7. *Oncogene* **22**, 5011–5020 (2003).
74. Elebro, K. *et al.* High estrogen receptor β expression is prognostic among adjuvant chemotherapy-treated patients—results from a population-based breast cancer cohort. *Clin. Cancer Res.* **23**, 766–777 (2017).
75. AdjoAka, J. & Lin, S.-X. Comparison of functional proteomic analyses of human breast cancer cell lines T47D and MCF7. *PLoS One* **7**, e31532 (2012).
76. Reed, B. G. & Carr, B. R. *The Normal Menstrual Cycle and the Control of Ovulation.* Endotext (MDText.com, Inc., 2000). <https://www.ncbi.nlm.nih.gov/pubmed/25905282>.
77. El-Sharkawy, H. *et al.* Platelet-rich plasma: Growth factors. *J. Periodontol.* **20**, 661–669. <https://doi.org/10.1902/jop.2007.060302> (2007).
78. Khetawat, G. *et al.* Human megakaryocytes and platelets contain the estrogen receptor beta and androgen receptor (AR): Testosterone regulates AR expression. *Blood* **95**, 2289–2296 (2000).
79. Nealen, M. L., Vijayan, K. V., Bolton, E. & Bray, P. F. Human platelets contain a glycosylated estrogen receptor beta. *Circ. Res.* **88**, 438–442 (2001).
80. Mezouar, S. *et al.* Involvement of platelet-derived microparticles in tumor progression and thrombosis. *Semin. Oncol.* **41**, 346–358 (2014).
81. Carey, L. A. *et al.* Race, breast cancer subtypes, and survival in the carolina breast cancer study. *JAMA* **295**, 2492 (2006).
82. El Sayed, R. *et al.* Endocrine and targeted therapy for hormone-receptor-positive, HER2-negative advanced breast cancer: Insights to sequencing treatment and overcoming resistance based on clinical trials. *Front. Oncol.* **9**, 510 (2019).
83. Chen, M. & Geng, J.-G. P-selectin mediates adhesion of leukocytes, platelets, and cancer cells in inflammation, thrombosis, and cancer growth and metastasis. *Arch. Immunol. Ther. Exp. (Warsz)* **54**, 75–84 (2006).
84. Reinert, T., Gonçalves, R. & Bines, J. Implications of ESR1 mutations in hormone receptor-positive breast cancer. *Curr. Treat. Options Oncol.* **19**, 24 (2018).
85. Leytin, V., Mody, M., Semple, J. W., Garvey, B. & Freedman, J. Flow cytometric parameters for characterizing platelet activation by measuring P-selectin (CD62) expression: Theoretical consideration and evaluation in thrombin-treated platelet populations. *Biochem. Biophys. Res. Commun.* **269**, 85–90 (2000).
86. BD FACSDiva™ Software|BD Biosciences-US. <https://www.bdbiosciences.com/en-us/instruments/research-instruments/research-software/flow-cytometry-acquisition/facsdiva-software>.
87. Olympus Soft Imaging Solutions. <https://www.olympus-sis.com/>.
88. Carpenter, A. E. *et al.* Cell profiler: Image analysis software for identifying and quantifying cell phenotypes. *Genome Biol.* **7**, R100 (2006).

Acknowledgements

The researchers thank the volunteers who donated blood for this study, the phlebotomist and staff at the Day Ward of the Charlotte Maxeke Academic Hospital, and Mrs E Miza for her assistance in the laboratory. The researchers thank the National Research Foundation of South Africa, Thuthuka Programme (NRF 87935 and 106926) (TNA) for funding.

Author contributions

Both authors contributed to the concept and design of the work. K.P. carried out experimentation with assistance from T.N.A. in acquisition, analysis and interpretation of the data. T.N.A. and K.P. drafted and approved the manuscript.

Competing Interest

The authors declare no competing interests.

Additional information

Supplementary information is available for this paper at <https://doi.org/10.1038/s41598-020-75779-y>.

Correspondence and requests for materials should be addressed to K.P. or T.N.A.

Reprints and permissions information is available at www.nature.com/reprints.

Publisher's note Springer Nature remains neutral with regard to jurisdictional claims in published maps and institutional affiliations.



Open Access This article is licensed under a Creative Commons Attribution 4.0 International License, which permits use, sharing, adaptation, distribution and reproduction in any medium or format, as long as you give appropriate credit to the original author(s) and the source, provide a link to the Creative Commons licence, and indicate if changes were made. The images or other third party material in this article are included in the article's Creative Commons licence, unless indicated otherwise in a credit line to the material. If material is not included in the article's Creative Commons licence and your intended use is not permitted by statutory regulation or exceeds the permitted use, you will need to obtain permission directly from the copyright holder. To view a copy of this licence, visit <http://creativecommons.org/licenses/by/4.0/>.

© The Author(s) 2020